Proceedings of the XVII ECSMGE-2019
Geotechnical Engineering foundation of the future
ISBN 978-9935-9436-1-3
© The authors and IGS: All rights reserved, 2019
doi: 10.32075/17ECSMGE-2019-0433

Test pumping and 3D hydraulic modelling – a deep excavation case study

Test de pompage et modélisation hydraulique en 3D – étude de cas d'une excavation profonde

Mats Kahlström

NGI, Oslo, Norway

Jürgen Scheibz(former), Siamak Feizi
NGI, Oslo, Norway

Martin Stormoen
BaneNor, Oslo, Norway

ABSTRACT: Confined aquifers in incised valleys are a typical geological feature in landscapes dominated by the influence of quaternary ice ages. Such conditions, a trench filled with glaciofluvial deposits, was encountered during the Ringerike line and E16 highway project in Norway. Two deep excavations, each 300 m long and 16-20 m deep, were planned to cross the trench in parallel. Concerns were raised regarding the potential for large hydraulic gradients and subsequent need for dewatering pumps. In order to reduce uncertainties, support the geotechnical evaluation and provide a basis for selecting the most suitable design, a full-scale aquifer-pumping test was performed to. Pumping was performed from two confined aquifers on the site, monitored by 20 electrical piezometers. Based on results from a transient 3D hydraulic Modflow model, simulating two groundwater-lowering scenarios, a scheme of eight dewatering pumps with a capacity between 160-350 m^3/day should be established during the construction phase in order to ensure stability against hydraulic failure of the excavations.

RÉSUMÉ: Les aquifères confinés dans les vallées incisées sont typiques des paysages dominés par l'influence des glaciations quaternaires. De telles conditions, avec une fosse remplie de dépôts glaciofluviaux, ont été rencontrées lors de la réalisation de la ligne de chemin de fer de Ringerike et de la route E16 en Norvège. Deux excavations parallèles et à ciel ouvert, chacune de 300 m de long et de 16 à 20 m de profondeur, devaient traverser la fosse. Des inquiétudes ont été exprimées concernant d'éventuels forts gradients hydrauliques et le besoin subséquent de pompes d'assèchement. Afin de réduire les incertitudes géotechniques et de fournir une base pour choisir la conception la plus appropriée, un test de pompage d'aquifère à grande échelle a été effectué. Le pompage a été réalisé dans deux aquifères confinés sur le site, monitoré par 20 piézomètres électroniques. Basé sur les résultats de modélisation hydraulique transitoire avec Modflow 3D simulant deux scénarios d'abaissement de la nappe phréatique, un système de huit pompes d'assèchement d'une capacité comprise entre 160 et 350 m3 / jour sera mis en place pendant la phase de construction afin d'assurer la stabilité de l'excavation.

Keywords: hydrogeology, aquifer pumping, Modflow, deep excavation

1 INTRODUCTION

Different potential heads between two sides of a deep excavation and the subsequent movement of water through pores within the soil body could trigger construction instability and affect system performance.

For two parallel deep excavation planned in southern Norway, initial site investigations raised concern related to the hydrogeological conditions and its possible impact on selecting the most feasible temporary support structure strategy. Further site investigation was performed and a full scale aquifer pumping tests was planned and executed in order to obtain a better understanding on the behavior of the two aquifers identified in the subsoil. A 3D numerical simulation with Modflow 2005 followed such that the influx of groundwater into the two excavations could be predicted, and establish a dewatering strategy.

Dewatering is an effective method to increase the construction stability by reducing the pore pressure. With dewatering, the water is extracted from the aquifer through number of wells. However, conventional well-point and deep well systems, commonly used for pumping water in coarse soils, are ineffective in fine soils, where vacuum well systems may be required (Preene, 1993, Cashman and Preene, 2013).

2 TWO DEEP EXCAVATIONS

As part of the Ringerike line and E16 highway project in Norway, a parallel highway and high-speed railway line will cross a deep trench consisting of glaciofluvial and glaciomarine soil deposits. Casting of the road and railway culverts are planned to take place in two adjacent deep excavations, each approx. 300 m long and between 16 to 20 m deep. Figure 1 illustrates a longitudinal cross-section of the trench crossing with a red line indicating the target road and railway level. The trench is today used as farm land with a small housing development along the southern edge.

2.1 Soil investigation and well installation

A series of field and laboratory tests were performed on the project site. Field work consisted of 51 Norwegian total soundings, 17 CPTU-soundings, 72mm undisturbed piston core samples, Sonic Drilling disturbed core samples and the installation of 20 electrical Geotech PVT piezometers. Two pumping wells and five observation wells were installed in the center of the trench, in between the two planned deep excavations.

Two of the observations wells were constructed with casing, filter medium and bentonite sealant. The piezometers for the remaining three observation wells were pushed down using a conventional geotechnical drill rig. The latter installation method was considerably faster and no distinguishable performance difference was registered between the well types during the pumping test.

2.2 Soil conditions

The general ground condition on site is presented in Table 1. The site consist of firm to stiff glaciomarine clay overlaying a fine to medium grained sand with interbedded silt and clay layers of variable thickness. A prominent layer of sandy silty clay within the sand deposit, unit IV, form two separate aquifers – an aquifer in unit III between 18 to 22 m depth and an aquifer in unit V between 22 m and bedrock level.

Table 1 Stratigraphy and hydrogeological classification.

Soil unit	**Top of layer (masl[1])**	**Soil type**	**Hydrogeological classification**
I	+94	Crust	-
II	+92	Clay	Unconfined aquitard
III	+79	Sand	Confined aquifer
IV	+76	Silty clay	Leaky aquitard
V	+72	Sand	Confined aquifer
VI	+50	Bed-rock	-

(1): masl = metres above sea level

The average measured pore pressure (red line) and the hydrostatic condition (as an index) is illustrated in Figure 2. The sand deposit is likely draining toward the lower-laying Tyrifjord in the west-end of the trench.

The bedrock consists of tightly folded interbedded claystone and limestone

Based on 25 sieve tests, the hydraulic conductivity K^{pred} of the upper and lower aquifer was estimated, as listed in Table 2.

3 FULL SCALE PUMPING TEST

Based on the result from a pumping test, hydrogeological properties such as hydraulic conductivity *K*, transmissivity *T* and storativity *S* can be determined. A well layout, as illustrated in Figure 3, was established consisting of two pumping wells, one for each aquifer, and five observation wells. Each observation well included three piezometers installed at 18 m, 26 m and 35 m depth respectively. One piezometer was also installed in each pumping well. The piezometers and electrical flow meter were connected to a remote monitoring system, providing real-time data logging and storage. At time $t < 15$ min, the data logging frequency was 60 s whereas at $t > 15$ min the frequency was 15 min.

Table 2 Predicted hydraulic conductivity using internal NGI method, K^{pred}, predicted and actual pumping rates.

Soil unit	**Well no.**	**K^{pred} (m/s)**	**Predicted max. output (l/s)**	**Actual max. output (l/s)**
III	1	9E-6 to 7E-6	0.25	0.22
V	2	9E-5 to 7E-5	1.0	1.97(1)

(1): Limited by pump system available on site, not aquifer capacity.

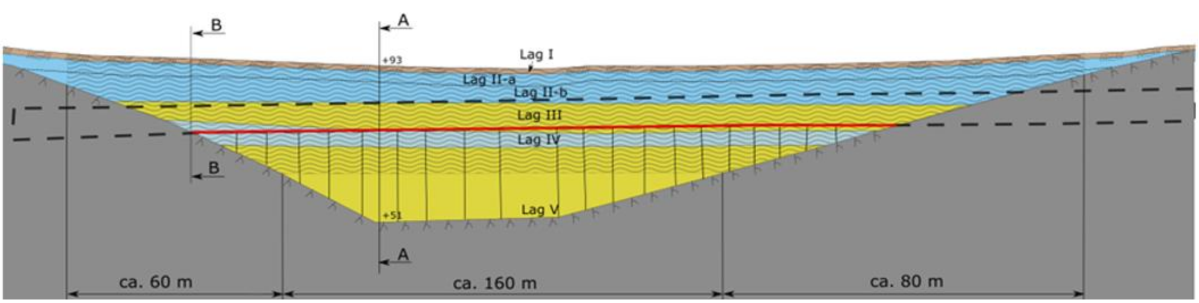

Figure 1 Longitudinal cross section across trench.

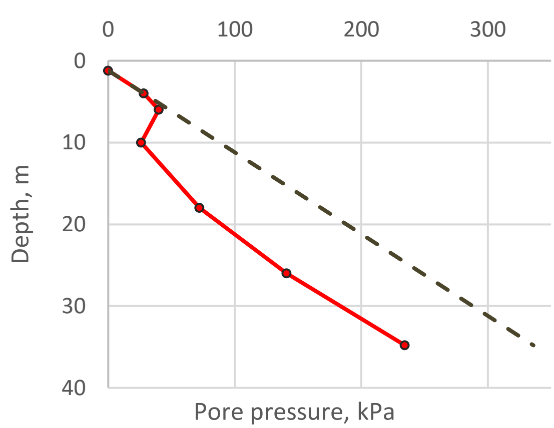

Figure 2 Measured average pore pressure vs depth.

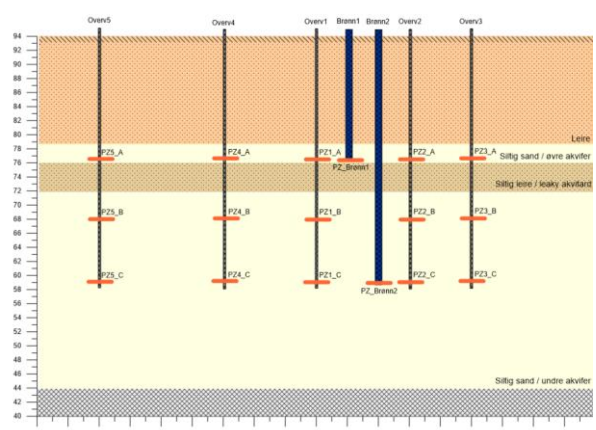

Figure 3 Well and instruments locations.

The maximum aquifer output was determined from the predicted K, as listed in Table 2, using a method by Theis (1935). After an initial surging phase, to wash out fines, the aquifer pumping test followed the steps as outlined by Fetter (2001), and shown in Figure 4**Error! Reference source not found.**. During the pumping test, using a Grundfos SQ-3-55 pump, the actual output corresponded well with the predicted output for the unit III aquifer. However, for the unit V aquifer, the actual output from well 2 had to be almost doubled, compared to the predicted output. In order to obtain a sufficient discharge in terms of aquifer drawdown the test was temporarily stopped (< 45 min) and a more powerful Grundfos SQE-7-40 pump system was installed.

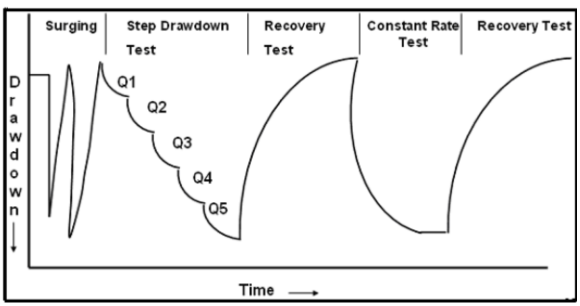

*Figure 4 The pump*ing concept (Fetter, 2001).

3.1 Step-drawdown test

In this step, the pumps starts with a low pumping rate, and then increases the rate stepwise for at least three steps until the maximum pumping rate is reached. The purpose of a step-drawdown test is to identify the highest pumping rate that can be used for a constant pump test. This also allows to identify the optimal depth deployment of the pump and to observe changes of piezometric pressure in the observation wells.

3.2 Constant rate test

A constant pump test is a continuation of a step-drawdown test that has achieved the maximum pumping rate. The maximum pumping rate is maintained at a constant level so that a stationary relationship with a constant sinking of the groundwater level is achieved. For confined aquifers it is common practice to perform constant pumping for at least 24 hours in order to assess boundary conditions.

3.3 Recovery test

Following the step-drawdown and constant pump tests, as shown in Figure 4, a recovery test is performed. The purpose of such a test is to monitor the pressure increase back to the initial groundwater level in the main experimental well and in the observation wells after the pumping is completed.

4 RESULTS - FULL SCALE TEST

Figure 5 shows the recorded pore pressures from the piezometers in the pumping and observation wells throughout the pumping test. A main finding is shown with inclined red arrows in figure 5, where a slight drawdown is observed in the aquifers although the pumping is performed in the other aquifer. It is therefore considered that unit IV (consisting of silty clay) is not impermeable, but instead exhibit a leaky behavior. As a consequence, the Theis (1935) solution is not considered suitable to describe the in-situ hydrogeological conditions present on site. Going forward, a solution formulated by Hantush and Jacob (1955) is adopted.

4.1 Pumping in well no. 1

Based on the field test data the hydraulic conductivity K^{pump} for the aquifer in soil unit III, from pumping in well no. 1, was determined to be in the range of 1.8 to 4.9E-06 m/s.

Figure 6 visualizes the drawdown over time for all wells in connection with the pumping test in well no. 1. Observed and calculated interpretation (black curve) drawdown show very little deviation. However, with time, an increasing discrepancy between observed and calculated drawdown is observed for well no. 1. This is interpreted as heterogeneity in soil unit III (sand) from dense silt and clay lenses affecting inflow to the well. This effect yields a deviation of 2.5 - 3.5% between the observed and interpreted drawdown.

4.2 *Pumping in well no. 2*

Figure 7 visualize the decay over time for well no. 2 and all five observation wells in connection with the pumping test in well 2. The hydraulic conductivity K^{pump} for soil unit V is determined to be in between 3.2 to 5.0 E-5 m/s.

It is noted that due to harsh weather conditions during the field works, no recovery test was performed in between the step drawdown and constant rate tests.

Table 3 Hydrogeological properties for the numerical simulations.

Soil unit	K^{pump} (m/s)	Porosity (%)	T (m^2/s)	S (-)
II	1.0E-9	40	-	-
III	3.4e-6	35	5.8E-5	1.9E-3
IV	1.0E-8	40	-	-
V	4.0E-5	30	6.8E-4	1.3E-3
IV	1.0E-6	10	-	-

5 NUMERICAL SIMULATIONS

A 3D model, with an area of 1 km^2, was designed to simulate a constant groundwater drainage to the excavations and assess the need for dewatering during the construction phase. Groundwater flow to the excavation was simulated with Modflow 2005 and the model is designed by means of Groundwater Modeling System Version 10.3 (based on Owens et al., 1996) as graphical surface.

LIDAR surveys and a combination of airborne electromagnetic survey, AEM, (Pfaffhuber et al, 2016) and geotechnical boreholes were used to create the terrain, soil and bedrock surfaces respectively.

Geophysical investigations, such as AEM, are a powerful tool to tie the gaps between individual boreholes, improving ground model accuracy. For example, AEM helped uncovering a bedrock high zone in the southern part of the modelling area, see figure 8, in an area where no geotechnical borings had been done. The lithological model accuracy is highest in the central parts, where a large number of geotechnical borings were performed.

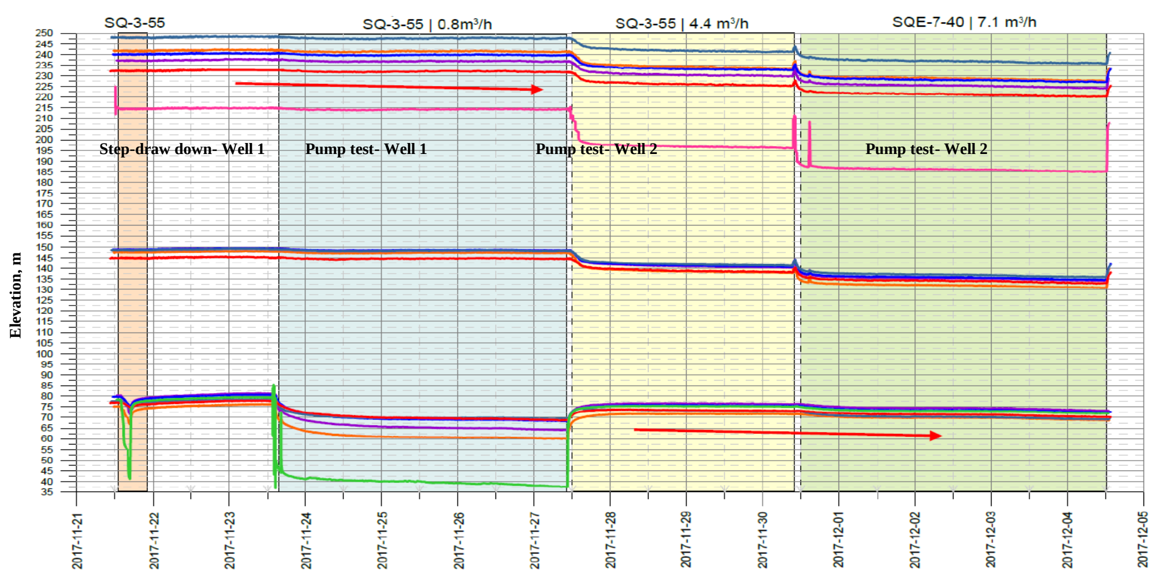

Figure 5 Time series of piezometers in observation wells and pump wells. Red arrows show a drawdown in an aquifer not currently subjected to pumping, indicating a leaky aquitard.

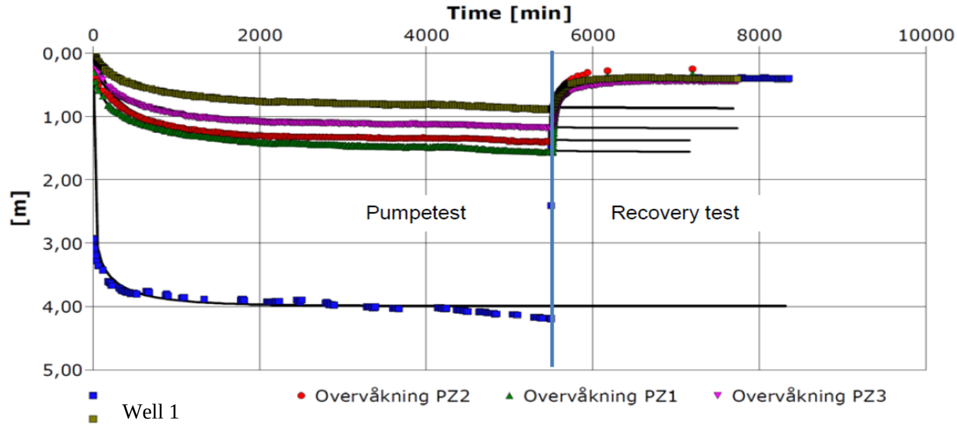

Figure 6 Visualization of the delay over time for Well 1 and observation wells PZ1-PZ5.

Both the stationary and transient model conditions were calibrated using observations available from the site, such as results from the pumping test. The maximum deviation is 0.7m, with a median of 0.25m for the non-calibrated model. This shows a good match between actual and modeled relationships and the concept model. *Input parameters for the 3D model are given in* Table 3 and an overview of the final model area for the 3D simulation is shown in Figure 10**Error! Reference source not found.**. The annual average rainfall in this area is 531 mm.

As a "solver" (mathematical program solving differential equations in Modflow), it was decided to use the Modflow NWT module (Niswonger et al., 2011), a Newton Formulation of Modflow 2005 (Harbaugh et al., 2005). The advantage of the NWT module is that it can handle dry cells, which was encountered in this model.

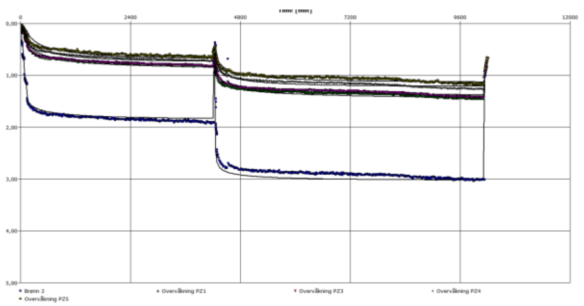

Figure 7 Visualization of the drawdown as function of time for well no. 2 and observation wells.

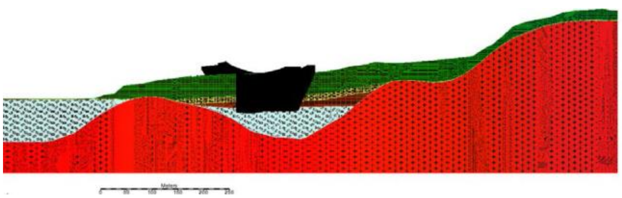

Figure 8 Cross section of the 3D model (see black dotted line in Figure 10 ***Error! Reference source not found.****).*

5.1 Results of dewatering simulations

In the numerical analysis, dewatering to +72 and +69 masl was performed using 8 wells placed adjacent to the sheet pile walls in order to investigate the required pumping capacity.

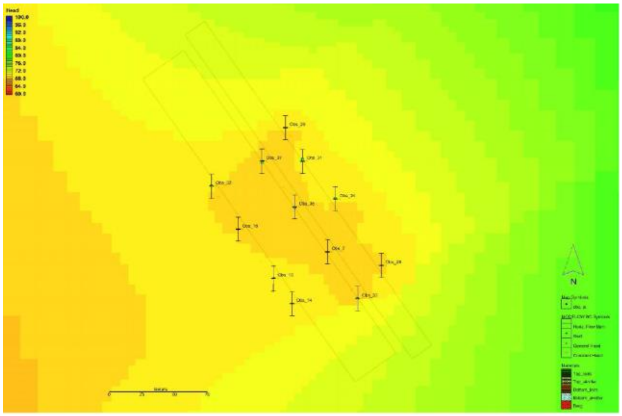

Figure 9 Water level around the expected excavation area (black lines) - Lowering to level +69.

The result is shown in Figure 9**Error! Reference source not found.** for dewatering down to +69 masl and the suggested well layout is shown in Figure 11.

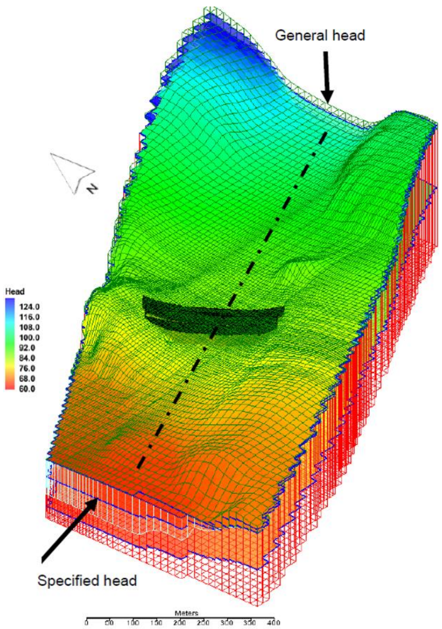

Figure 10 3D model, black hatch show the two deep excavations across the trench.

Table 4 provides the simulated required pumping rates for each dewatering well in order to obtain the specified groundwater lowering. Flow rates are greatest in the central parts of the model where depth to bedrock is the largest.

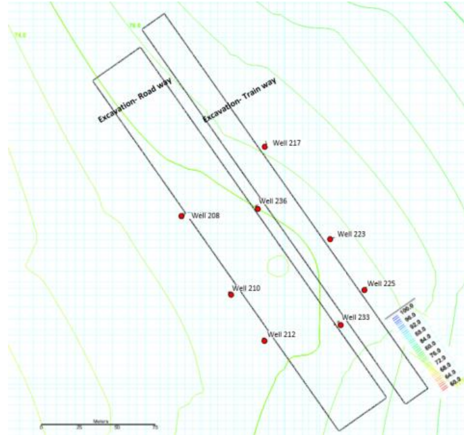

Figure 11 Location of eight dewatering wells (red dots) adjacent to the two planned deep excavations.

Table 4 Flow rates from the dewatering simulation.

Dewater-ing well	Dewatering to +69 (m^3/day)	Dewatering to +72 (m^3/day)
208	1.6	0.1
210	1.4	16.8
212	1.9	8.7
217	50.5	64.8
223	135.3	60.2
225	66.6	56.7
233	7.8	39
236	56.3	44.9

Further, a simulation was performed using the ZoneBudget program (Harbaugh et al., 1990) in order to estimate the amount of free-flow water into the fully excavations in case of no pumping. The free flow is expected to be approx. 160 m^3/day for each pit.

6 CONCLUSIONS

For large excavations in complex geological conditions, reducing uncertainty related to the potential for failures associated with large hydraulic gradients is important. A full scale pumping test is a powerful tool in order to determine hydrogeological properties, not readily interpreted only from geotechnical site investigations.

For this project, such a full-scale test was performed using a large number of electrical piezometers. Based on the pumping test results, a 3D hydraulic model was established. The model showed that the assumptions drawn from only geotechnical investigations and sieve curves would have been insufficient to properly determine the in-situ hydraulic conditions. During pumping from well no. 2, as detailed in Table 2, the water pump had to be replaced in order to facilitate a significantly higher pumping rate than what was expected based only on sieve curve results.

The 3D Modflow model was then used to simulate two dewatering scenarios below the bottom of the excavations. While the validation of the model showed a good fit between observed and numerical results, the boundary conditions include a rather large degree of uncertainty. It is therefore recommended to include a reserve budget in the dewatering pump capacity in order to account for this uncertainty. It is recommended that the dewatering wells should have a capacity of between 160-350 m^3/day, taking into account local variation in flow conditions.

7 REFERENCES

Cashman, P.M., and Preene, M., 2013, Groundwater lowering in construction: A practical guide to dewatering, *CRC Press*, New York, London, hardback, 645 pp.

Fetter, C.W., 2001, Applied Hydrogeology (4th ed.), Prentice-Hall, Upper Saddle River, New Jersey, 598p.

Hantush, M.S., 1960. Modification of the theory of leaky aquifers, *J. Of Geophys. Res*., vol. 65, no. 11, 3713-3725.

Harbaugh, A.W., 1990, A computer program for calculating subregional water budgets using results from the U.S. Geological Survey modular three-dimensional ground-water flow model, U*.S. Geological Survey Open-File Report*, 90-392

Harbaugh, A. W., 2005, MODFLOW-2005, the US Geological Survey modular ground-water model, *the ground-water flow process*, Reston: US Department of the Interior, US Geological Survey.

Neuman, S.P. and P.A. Witherspoon, 1969. Theory of flow in a confined two quifer system, *Water Resources Research*, vol. 5, no. 4, 803-816.

Niswonger, R.G., Panday, Sorab, and Ibaraki, Motomu, 2011, MODFLOW-NWT, A Newton formulation for MODFLOW-2005: *U.S. Geological Survey Techniques and Methods*, 6-A37.

Owens, S. J., Jones, N. L., & Holland, J. P., 1996. A Comprehensive Modeling Environment for the Simulation of Groundwater Flow and Transport, *Engineering with Computers*, 12.3-4, 235-242.

Preene M., 1993, Case studies of construction dewatering in fine grained Eocene soils, *Ground Engineering*, 23-26.

Theis, C.V., 1935. The relation between the lowering of the piezometric surface and the rate and duration of discharge of a well using groundwater storage, *Am. Geophys. Union Trans.*, vol. 16, 519-524.

Pfaffhuber, A., Anschütz, H. & Kåsin, K. 2016. The Emperor's New Clothes—Opportunities and Limitations Applying AEM to Geotechnical Design Work. *25th International Geophysical Conference and Exhibition (pp. 372-376)*